

The myth of the molecular ring

C. L. Dobbs^{*1,2,3} and A. Burkert^{1,2†}

¹ *Max-Planck-Institut für extraterrestrische Physik, Giessenbachstraße, D-85748 Garching, Germany*

² *Universitäts-Sternwarte München, Scheinerstraße 1, D-81679 München, Germany*

³ *School of Physics, University of Exeter, Stocker Road, Exeter EX4 4QL*

24 March 2021

ABSTRACT

We investigate the structure of the Milky Way by determining how features in a spatial map correspond to CO features in a velocity map. We examine structures including logarithmic spiral arms, a ring and a bar. We explore the available parameter space, including the pitch angle of the spiral arms, radius of a ring, and rotation curve. We show that surprisingly, a spiral arm provides a better fit to the observed molecular ring than a true ring feature. This is because both a spiral arm, and the observed feature known as the molecular ring, are curved in velocity longitude space. We find that much of the CO emission in the velocity longitude map can be fitted by a nearly symmetric 2 armed spiral pattern. One of the arms corresponds to the molecular ring, whilst the opposite arm naturally reproduces the Perseus arm. Multiple arms also contribute to further emission in the vicinity of the molecular ring and match other observed spiral arms. Whether the Galactic structure consists primarily of two, or several spiral arms, the presence of 2 symmetric logarithmic spirals, which begin in the vicinity of the ends of the bar, suggest a spiral density wave associated with the bar.

1 INTRODUCTION

Despite decades of observations, determining the spiral structure of our Galaxy is still intrinsically difficult. It is not even clear whether the Galaxy contains 2, 3 or 4 primary spiral arms (Vallée 2005, 2008; Benjamin 2008; Steiman-Cameron et al. 2010), and whether the spiral structure is different in the gas and the stars. Traditionally, much of the CO emission of the Galaxy has been associated with a feature known as the ‘molecular ring’ (Stecker et al. 1975; Cohen & Thaddeus 1977; Roman-Duval et al. 2010), around 4 kpc from the Galactic Centre. However it is unclear whether this is truly a ring, or simply emission from nearby spiral arms, as suggested by simulations of spiral galaxies (Englmaier & Gerhard 1999; Rodriguez-Fernandez & Combes 2008; Baba et al. 2010).

In the past, the spiral structure for the Galaxy has predominantly been determined from the stellar distribution (Vallée 2005 and references therein). Measuring distances to stars is difficult for distances larger than a few kpc however due to extinction. Alternatively we can use a gas tracer such as CO or HI. In other galaxies, e.g. M83, M51, the spiral arms also tend to be much narrower in the gas than the stars, indicating that gas is likely a better tracer of spiral structure. For a spiral density wave, the gaseous and stellar spiral arms are expected to occupy slightly different patterns, with the gaseous arms slightly offset from the stellar arms except at corotation, and with a smaller pitch angle (Gittins & Clarke 2004)¹. The gaseous structure is also much more complex

than the stellar, with interarm spurs, and branches between spiral arms absent in the stellar distribution.

CO and HI maps of the Galaxy (e.g. Dame et al. 2001) clearly show the Perseus and Outer arms. However there are also difficulties with using gas tracers: i) it is difficult to map the opposite side of the Galaxy, ii) the emission in the inner part of the Galaxy is dominated by a broad band in velocity-longitude (hereafter $l-v$) space, and iii) ambiguities in calculating the distance to gaseous features from the rotation curve and velocity crowding. Thus mapping the spatial structure from the gas is far from straightforward.

In this paper we take a slightly different approach. Rather than using the molecular emission, or stellar distribution, to estimate the spiral structure, we instead assume the gaseous spiral arms exhibit some pattern and see how well they fit the observed CO emission. We do not perform numerical simulations rather we simply assume the gaseous spiral arms follow a logarithmic spiral pattern, assumed to arise from the gas response to a density wave. This has the caveat that our results neglect streaming motions. However if we can fit the spiral pattern even in the absence of streaming motions, this is a strong indication that the spiral pattern for our Galaxy can be represented by a simple $m = 2$ or $m = 4$ pattern. There are also two direct advantages of our method; the first that we can readily explore a large parameter space, and the second that we do not need to include the pattern speed, or spiral potential strength, which are unknown parameters. A similar approach has been carried

that for a kinematic wave driven by a tidal interaction, the stellar and gaseous arms are not systematically offset.

¹ although recent simulations of M51 (Dobbs et al. 2010) find

out by Russeil (2003) for star forming complexes, but the distribution they use does not display strong spiral structure. Steiman-Cameron et al. (2010) also fit spiral patterns to the intensity of FIR cooling lines at each position in the Galaxy.

2 METHOD

To obtain spiral arms, we assume that the molecular gas lies in a 2 or 4 armed logarithmic spiral pattern. From standard density wave theory, the general expression for a logarithmic spiral pattern is

$$\phi = A(r) \cos\left(\frac{n}{\tan i} \log(r/r_0) - (\theta - \Omega_p t)\right) \quad (1)$$

where $A(r)$ provides the amplitude of the spiral, n is the number of spiral arms, i is the pitch angle, r_0 is a constant which controls the orientation of the arms, and Ω_p the pattern speed. Since we only require the pattern at the present time, we can set $t = 0$. To find the minima of the potential, we then simply have

$$\frac{n}{\tan i} \log(r/r_0) = \theta, \quad (2)$$

and given some values of i and r_0 we can map the positions of the spiral arms.

We then compute the velocity longitude map, requiring a given rotation curve. We adopt a flat rotation curve for a logarithmic potential (Binney & Tremaine 1987), of the form

$$v = v_0 r^2 / (R_c^2 + r^2) \quad (3)$$

where v_0 and R_c are constants. R_c determines how far from the centre of the Galaxy the rotation curve becomes flat. Past observations have indicated the rotation of the Galaxy is between 210 and 240 km s⁻¹ over the majority of the Galaxy (Clemens 1985). The standard reference is $\Theta_0 = 220$ km s⁻¹ at $R_0 = 8$ kpc. However more recent measurements of the distance to masers suggest that Θ_0 may be 250 km s⁻¹ or higher (Reid et al. 2009). We tried both $v_0 = 220$ and 250 km s⁻¹, though we only show results for $v_0 = 250$ km s⁻¹. As the observations show that the velocity curve is still very high close to the centre of the Galaxy, we choose $R_c = 0.1$ kpc. Then we place the observer a distance of 8 kpc from the centre of the Galaxy.

We show results where we adopt a spiral arm pattern, and where we assume that the molecular ring is truly due to a ring. Given that we simply use the computed locations of the spiral arms, or ring, we can investigate a large parameter space. The free parameters in our models are the pitch angle of the spiral arms; the radius of a ring feature; the orientation of the spiral arms, the length and orientation of the bar; the Galocentric radius and the rotation velocity v_0 . We mainly consider the orientation and pitch angle of the spiral arms, but we also briefly mention the other parameters. In principle, this analysis could be carried out without any prior knowledge of the structure of the Milky Way, but given the large parameter space we have started with the location of the observer, the rotation curve, and the orientation of the bar roughly based on observations.

2.1 Fitting technique

We can compare how well our models match the CO observations by matching features such as the molecular ring, Perseus Arm, Outer Arm simply by eye. However we also carry out a χ^2 fitting between the velocity longitude map of Dame et al. (2001) and our models. The difficulty of the latter is that we have to make numerous assumptions to convert our models into emission maps. We assume the emission follows a Gaussian centred on the proposed spiral arms with a velocity dispersion of 7 km s⁻¹. We also have to make some assumptions about how the emission scales with radius. We suppose the intensity falls with $1/r_{LSR}^2$ where r_{LSR} is the distance to the local standard of rest (located at $R = 8$ kpc). We also assume that the amount of molecular gas falls off as $1/r_{GAL}$ where r_{GAL} is the radius of the Galaxy. We then normalise the emission so that the total emission matches that of Dame et al. (2001). We calculate the difference between the observed and model emission, $\sigma^2 = (I_{obs} - I_{mod})^2$, and minimise over the spiral arm orientation or molecular ring radius. Whilst departures from these assumptions (e.g. a different velocity dispersion, changes in scaling with r_{LSR} and r_{GAL}) change σ , how well the models fit relative to each other does not change.

There are still some difficulties with our fitting process when we compare to spiral features. In the Galaxy, local emission is present at all longitudes, but absent in our models. Away from the Galactic Centre, this emission dominates over features such as the Outer Arm. Thus we cannot really test for these features without introducing some arbitrary weighting, so we instead restrict our fit to longitudes between 50° and -50°. We still found however that this method was biased towards lower pitch angles, simply because the arms cross the region $l = \pm 50^\circ$ multiple times. Therefore we also carried out a fit just to the part of the main spiral arm which coincides with the molecular ring. We refer to the two fits as ‘total’ (i.e. for all the parts of the arms in our models between $l = 50^\circ$ and -50°) and ‘arm’ (i.e. just between the tangent points of the arm which coincides with the molecular ring).

In the first part of the results we compare a 2 armed and 4 armed spiral pattern, so we use the ‘total’ fit. In Section 3.1 we vary the pitch angle and compare results with both the ‘total’ and ‘arm’ fits. The best fit orientation of the arm does not depend on which technique is used, but the pitch angle does.

3 RESULTS

In Figure 1 we show our best fit to the molecular ring for a 2 armed spiral pattern (top panel) adopting a pitch angle of 11° (see next section for results with different pitch angles). This model includes a bar of radius 3 kpc, which we have simply placed across the Galactic centre 45° clockwise from the position of the Sun. In all figures, we simply show the lines tracing peak emission along the arms, rather than our synthetic emission maps. The lines are overplotted on the velocity longitude map of Rodriguez-Fernandez & Combes (2008), which used the data of Dame et al. (2001).

From Figure 1, top panel, we see that the Scutum-Centaurus (hereafter Sct-Cen) arm provides a good fit to

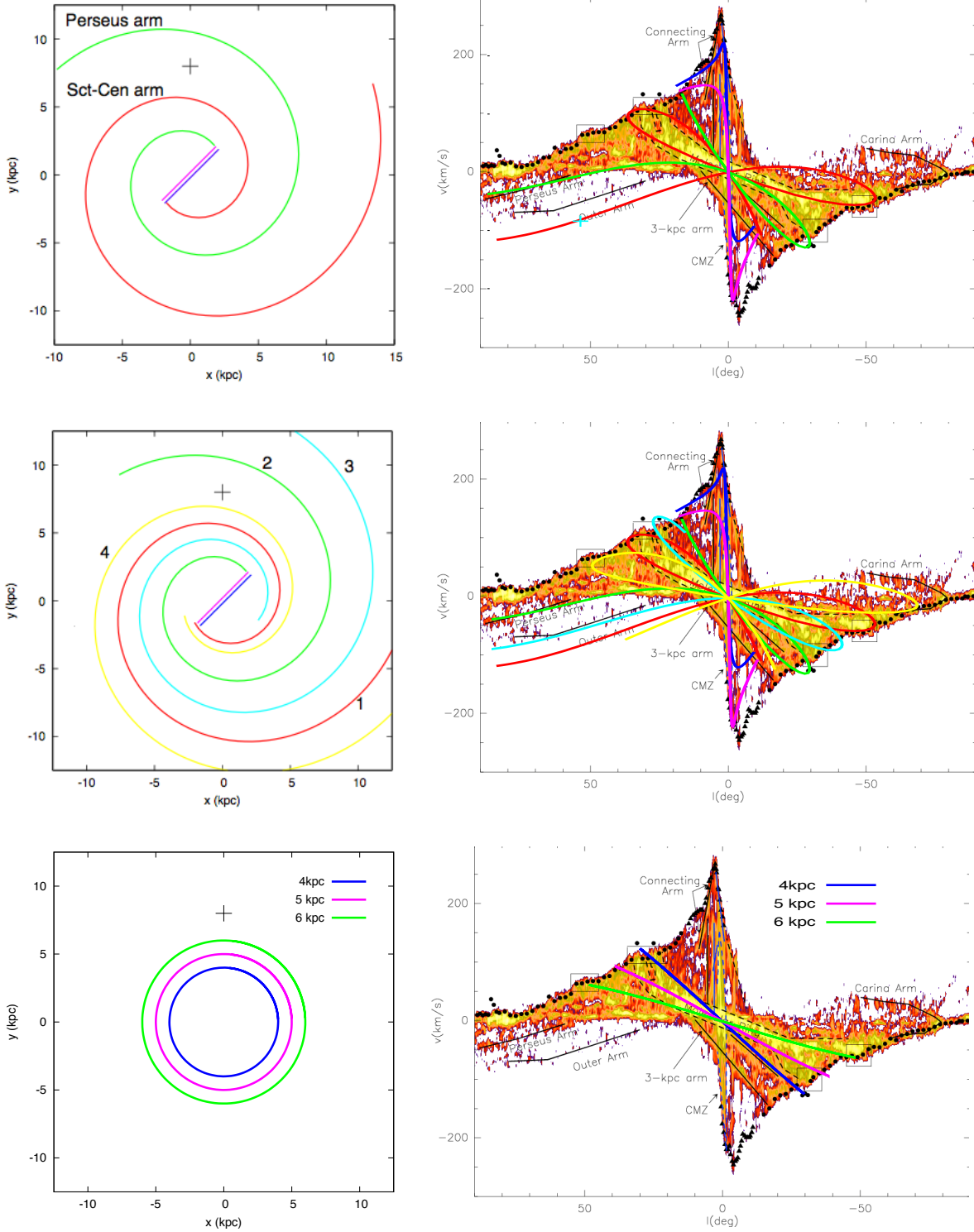


Figure 1. On the left hand side we illustrate possible Galactic features, a 2 armed spiral pattern (top), a 4 armed spiral pattern (centre) and 3 rings of different radii (lower). The position of the observer is marked by the cross at 8 kpc. On the right hand panels we show the location of the spiral arms in a velocity longitude plot, from Rodriguez-Fernandez & Combes (2008) who used the data of Dame et al. (2001). The black circles and crosses indicate terminal velocity measurements. The cyan cross shown in the top right panel indicates the extremity of the outer HI arm observed by Dame & Thaddeus (2011). The pitch angle for the spiral models is 11° . The spiral patterns are the best fit patterns (with regards to the orientation of the arms) to the observed emission between $l = \pm 50^\circ$. The Scutum-Centaurus arm provides a good fit to the molecular ring. The best fit ring has radius 6 kpc. However since the spiral arm is curved in $v - l$ space, it has a better fit to the molecular ring compared to a ring. Please view journal online for colour versions of the figures.

the molecular ring. The part of this arm in the lower left quadrant (negative l and v) also agrees very well with the location of the new arm as measured in HI by Dame & Thaddeus (2011). As also noted in their paper, it is very difficult to get the Sct-Cen arm to continue to the Outer arm, without providing a very asymmetric spiral pattern. The second spiral arm provides a good fit to the Perseus arm. The best fit for the second arm was almost symmetric with the Sct-Cen arm, only asymmetric by 10° . It is possible to rotate the arms slightly and produce better matches to the tangent points (boxes), still matching the spiral arms reasonably well, but here we simply show the best results to our molecular ring fitting technique. The emission from the second spiral arm (green) extends a little outside the scope of the observed CO emission. With a lower rotation curve ($v = 220 \text{ km s}^{-1}$), this is avoided. Otherwise there is little difference for a lower rotation curve.

It is difficult to constrain the starting radius of the Sct-Cen Arm, given the complex emission towards the Galactic Centre. We can however see that the arm marked as the Perseus arm cannot extend much further inward, else there would be unobserved emission (at $l \sim 15^\circ$, $v \sim 150 \text{ km s}^{-1}$) for this model.

In the centre panels of Figure 1 we show a 4 armed spiral model. To the two armed model, we added a third arm (cyan) using our fitting technique. This arm naturally reproduces the Outer arm emission. We tried adding a 4th arm, however our fitting technique did not show any minimum in the expected vicinity. Since this arm is close to the Sun (or observer), the emission, and therefore results became dominated by this arm, whereas for the observations, the strongest emission coincides with the molecular ring. Therefore we reduced our calculated emission from this arm by a factor of 10 compared to the other arms to fit the fourth arm. This arm then reproduces the Carina arm, and also the tangent point at $l \sim 50^\circ$, $v \sim 50 \text{ km s}^{-1}$. The factor of 10 is somewhat arbitrary but does seem to indicate that any arm between the Sun and the Sct-Cen arm is somewhat weaker. Overall though, the addition of extra arms superimposed on the Sct-Cen arm contribute further to the emission of the molecular ring.

In the lower panels of Figure 1 we show the results for rings. We show 3 examples with radii of 4, 5 and 6 kpc. It can be seen from Figure 1 that a ring does not cover as much of the emission of the observed ‘molecular ring’ as a spiral arm. The reason for this is because the observed molecular ring is actually curved in $v - l$ space, whereas the emission from an actual ring is a straight line. So we see that whilst a 4 or 5 kpc radius ring can fit emission for positive longitudes, it misses the emission at negative longitudes. Conversely, a 6 kpc ring reproduces the observed emission at negative longitudes, but does not agree with the brightest observed emission at positive longitudes. From our fitting technique, the 6 kpc ring gave the best fit, although by eye 5 kpc appears best (the difference is probably because the observed emission extends further at negative longitudes compared to positive longitudes).

In Table 1 we show the difference between the model estimated CO emission and that of the observations, $\sigma^2 = (I_m - I_{obs})^2$ for 1 (corresponding to the Sct-Cen arm in Figure 1), 2 (upper panels, Figure 1) and 4 (middle panels, Figure 1) armed spiral models with a pitch angle of 11°

Model	σ^2/σ_{4arm}^2
Ring	2.27
1 armed spiral	2.02
2 armed spiral	1.33
4 armed spiral	1.0

Table 1. The difference between the observed and analytic emission, σ^2 , where $\sigma^2 = (I_m - I_{obs})^2$ is shown for the ring model, and spiral arm models with a pitch angle of 11° . The 1 armed model refers to just the Sct-Cen arm in Figure 1. The results are normalised to our best fit model, the 4 armed spiral. The 4 armed spiral provides the best fit, though all cases are a better fit compared to a ring.

Pitch angle ($^\circ$)	σ^2/σ_{4arm}^2 (‘total’)	σ^2/σ_{4arm}^2 (‘arm’)
8.5	2.00	2.13
11	2.02	2.08
13.5	2.11	2.06
16	2.18	2.01

Table 2. We show the difference between the observed and analytic emission, σ^2 , where $\sigma^2 = (I_m - I_{obs})^2$ for the Sct-Cen arm with different pitch angles. For the left column, we consider emission along the total length of the arm. For the right column, we consider emission only between the tangent points of the Sct-Cen arm. The results are normalised as for Table 1. The best fit pitch angle is dependent on the fitting technique, however in all cases, the fit is better compared to a ring (Table 1).

and a ring of 6 kpc radius. The spiral models provide better fits statistically compared to the ring model. The 2 and 4 armed spirals are also better fits compared to the 1 armed model or ring, which is not surprising because they allow more complexity and cover a larger area where the observed emission lies. However distinguishing between the 2 and 4 armed models (and allowing for the different degrees of freedom) is probably beyond the scope of our approach.

We also performed a simpler test to compare between our models and the observed CO emission only between the tangent points of the Sct-Cen arm (the ‘arm’ fit). This test corrects for any bias due to spiral arms crossing the region $l = \pm 50^\circ$ multiple times. We show the results in Table 2, and again the spiral arm models still provide better fits compared to the ring.

3.1 Parameter study

In this section, we investigate how altering the parameters of our models affects how well the spiral arms fit the observed emission.

The main parameter which we can vary is the pitch angle of the spiral arms. In Figure 2 we show models with pitch angles of 8.5° , 13.5° and 16° . From Figure 2 we see that in all cases the molecular ring is well reproduced. Again, these are our best fit models, where we have fitted for the orientation of the arms. Thus to a large extent there is a degeneracy between the pitch angle and the orientation of the arms, though it is not always possible to reproduce other Galactic features.

For the pitch angle of 8.5° , we obtain a very asymmetric

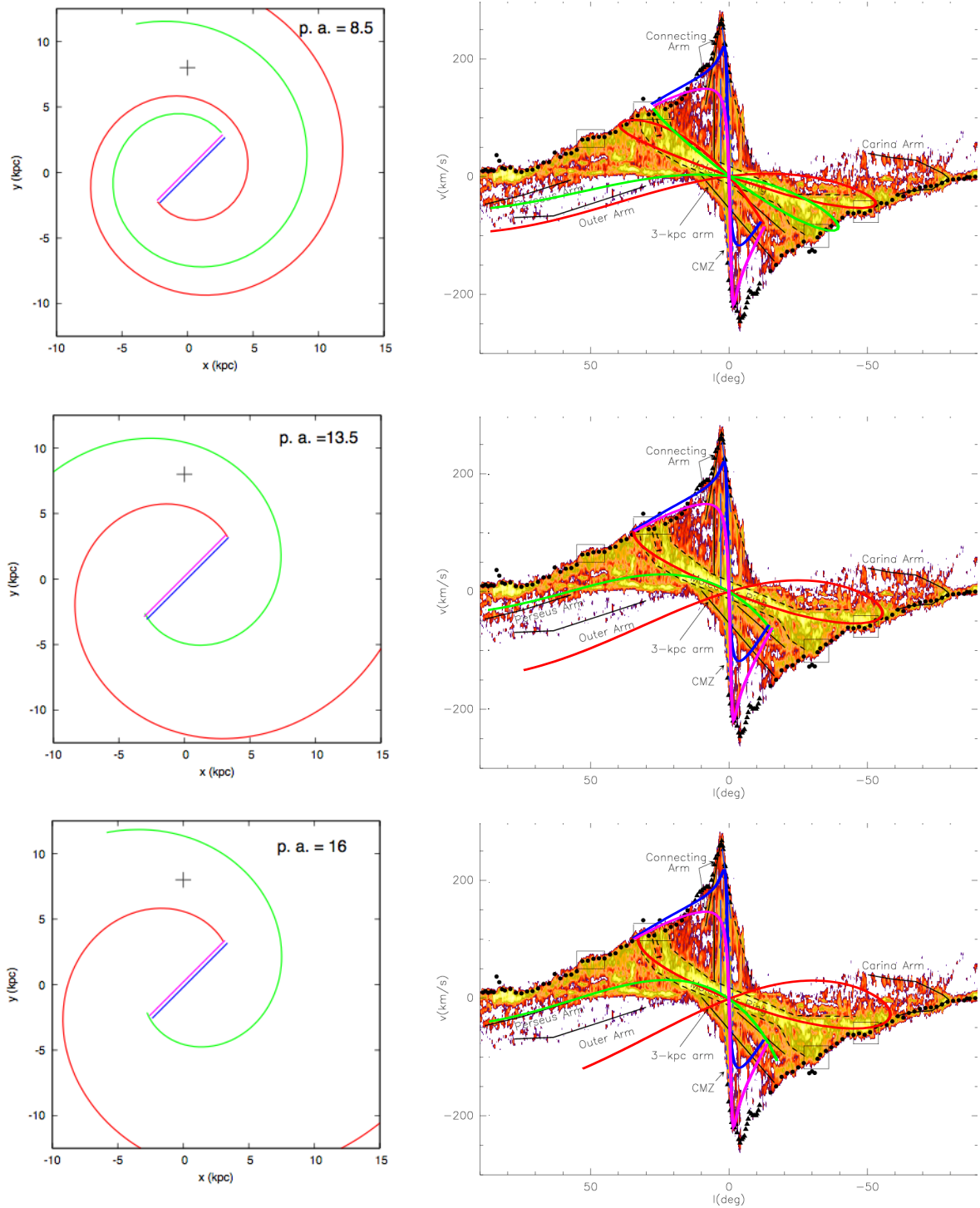


Figure 2. The spiral pattern is shown for models with 2 spiral arms and pitch angles of 8.5° (top), 13.5° (centre) and 16° (lower). The position of the observer is marked by the cross at 8 kpc. The arms have been rotated to provide a best fit to the data. In all cases the Sct-Cen arm easily fits the molecular ring. For a pitch angle of 8.5° , there is a good agreement with the observed CO emission, but the spiral arms are highly asymmetric. For higher pitch angles, we do not reproduce the tangent point at $l = 30^\circ$, $v = -100 \text{ km s}^{-1}$ as the arms do not extend to the inner part of the Galaxy, and also it is difficult to reproduce this tangent point and the Perseus arm simultaneously. Please view journal online for colour versions of the figures.

pattern. Our fitting technique does not take into account tangent points, or the Perseus arm which are also constraints on the second spiral arm (green). However even if we adjust the second spiral to fit the tangent point at $l \sim -30^\circ$, $v \sim -100 \text{ km s}^{-1}$, the structure is still highly asymmetric.

For pitch angles of 13.5° and 16° we do not produce the tangent point at $l \sim -30^\circ$, $v \sim -100 \text{ km s}^{-1}$ simply because the emission does not extend that far inwards. We could continue the arms for another half rotation, however this would lead to a rather short ($\lesssim 2 \text{ kpc}$) bar, with the assumption that the arms begin at the bar. In any case it is difficult to match the tangent point and the Perseus arm simultaneously, especially when the pitch angle is 16° . Another constraint is the observed distance to the Perseus arm, which is around 2 kpc towards $l = 134^\circ$ (Xu et al. 2006). We get good agreement with this for the models we present. However if we constrain the Perseus spiral arm to match the the tangent point at $l \sim -30^\circ$, $v \sim -100 \text{ km s}^{-1}$, the distance to the Perseus arm becomes too large for the higher pitch angles. Finally we note that we do not get good agreement with the newly observed outer HI arm (Dame & Thaddeus 2011) with these pitch angles, in particular 8.5° and 16° .

We show in Table 2 how well the models with different pitch angles fit the observed data, using the ‘total’ and ‘arm’ fits. The ‘total’ fit favours lower pitch angles, because the arms cover more of the region of observed emission. The ‘arm’ fit favours larger pitch angles, and provides a best fit pitch angle of 16.5° . Both techniques however neglect features such as the Perseus arm, outer HI arm, and supposed tangent points, which appear necessary to constrain the pitch angle. With these extra constraints, the 11° pitch angle reproduces more of the CO features.

We also tested the orientation of the bar, the rotation curve and the position of the observer in the Galaxy. As noted before, decreasing the rotation curve to 220 km s^{-1} slightly reduces the scope of the emission in velocity space. Moving the radius of the observer closer to the Galactic Centre increases the span of the nearer spiral arm in the velocity plot. Thus to still achieve a similar pattern to Figure 1, a lower pitch angle would be required, and likewise if the observer is further out in the Galaxy, a higher pitch angle would be needed. So again there is a degeneracy between the Galocentric radius and the pitch angle, but again, with significant departures from the observed values, it is more difficult to reproduce all the features in the CO map simultaneously.

Changing the orientation of the bar does not make a very noticeable difference to the location of emission associated with the bar. It is difficult to reproduce the full extent of CO emission in velocity space associated with the bar, i.e. for velocities in excess of $+200 \text{ km s}^{-1}$. This could be due to a higher rotation curve, motions along the bar, or simply features near the Galactic Centre that we are missing.

3.2 Comparison to other models of the Milky Way

There have been several models suggested for the structure of the Milky Way in recent years. Vallée (2005) proposes a 4 armed spiral model with a pitch angle of 12° . The main difference between his model, and our 4-armed model is that we suppose that the Perseus and Scutum-Centaurus Arm

start at the bar, whereas Vallée (2005) assumes that the Sagittarius-Carina and Cygnus (Outer) Arms start at the bar (these are the equivalent to the arms coloured cyan and yellow on Figure 1). We constrained the models such that the Scutum-Centaurus and Perseus Arm begin at the bar, because these arms are seen in the stars and the gas, whereas the other arms may not be associated with stellar enhancements (Drimmel 2000; Benjamin 2008).

Churchwell et al. (2009) also proposed a schematic of the Galaxy based on the GLIMPSE infrared survey (see also Benjamin 2008). They propose that the Galaxy is a 2-armed spiral, the main arms being the Scutum-Centaurus and Perseus Arms, with several secondary spiral arms. They adopt a long bar, but do not state the pitch angle of the arms. This is similar to our 11° pitch angle model if we choose a longer bar, and neglect the first 180° rotation of the spiral arms, or the models we show for larger pitch angles. We did note though in Section 3.1 that starting the arms further out in the disc would likely miss regions of emission in the CO $l-v$ diagram.

Finally, Steiman-Cameron et al. (2010) propose a model based on [CII] and [NII] cooling lines. This is very similar to our 4 armed model in Figure 1. The main difference is that they use slightly larger pitch angles ($13 - 16^\circ$), and whilst we obtained a reasonable fit with one pitch angle, they used different pitch angles for each arm. With the pitch angle for the Scutum-Centaurus arm they used (15.5°), it is difficult to reproduce the HI feature seen by Dame & Thaddeus (2011) as the arm barely extends to the third Galactic quadrant.

4 DISCUSSION

It is relatively easy to find a spiral arm configuration such that the region corresponding to the molecular ring is reproduced by a nearby spiral arm. If we rotated the nearest spiral arm (with respect to the Galactic Centre), we would obtain a similar feature with a different gradient. Increasing or decreasing the pitch angle of the arms changes the extent of the molecular ring. Other spiral arms enhance the molecular ring, as all overlap at least at $l = 0$. Finally, as the molecular gas surface density decreases with radius, outside the vicinity of the bar, the maximum emission will be from the near spiral arm close to the bar.

Whilst a ring feature can also represent CO emission similar to the observed molecular ring, a ring does not fit the observations as well as a spiral arm. This is because the spiral arm appears curved in $v-l$ space, similar to the observed molecular ring, but dissimilar to a true ring. Thus whilst we cannot rule out that the molecular ring corresponds to a true ring, we found that a spiral arm produced a better fit compared to a ring over all our range of pitch angles, and this finding was robust to the details of our fitting technique.

Binney et al. (1991) proposed that the molecular ring could be due to the outer Lindblad resonance of the bar. We also performed simulations with a barred potential to examine whether a gaseous ring would form. However generally gas features produced at the end of the bar are highly elliptical, as seen already in numerical simulations (e.g. Wada & Norman (2001); Lin et al. (2008)). The elongated features

due to the bar in our Galaxy may well correspond to the far and near 3 kpc arms, seen in the molecular gas data. In our simulations of bars, any feature corresponding to a ring was again simply the spiral arms close to the Galactic centre. In fact, few galaxies show obvious rings in the gas at the end of the bar – typically rings are nuclear rings much nearer to the centre, or features caused by large collisions. Our Galaxy is probably not unusual in this respect.

Our fiducial model adopts a pitch angle of 11° , assuming a Galocentric distance of 8 kpc. All the pitch angles we tried could reproduce a feature similar to the molecular ring, and from fitting the molecular ring alone we find a best fit pitch angle of 16.5° . However deviations from the 11° model tend to reproduce fewer of the other observed features in the CO $l-v$ diagram, or produce highly asymmetric arms. Larger pitch angles seem to point towards a longer bar, which means CO in the lower right quadrant of the $v-l$ plot is absent. Moreover the supposed tangent point of the inner part of the Perseus arm, and the distance to the Perseus arm, cannot be matched simultaneously with large pitch angles. Our 2 armed spiral model is fairly symmetric, and is thus consistent with a density wave originating at the bar. Though we cannot rule out that the Galaxy simply consists of several, asymmetric, spiral arms, it seems less likely that by coincidence they match both the inner and outer spiral structure simultaneously. Reproducing all the features in the CO, e.g. Outer Arm, Carina Arm, requires 4 spiral arms.

It is thought that the Galaxy may exhibit two spiral arms which are evident in both stars and gas, whilst other features, e.g. the Sagittarius Arm, are only seen in the gas (Drimmel 2000; Benjamin 2008). The next step would be to try and produce hydrodynamical models with potentials based on the 2 armed spiral pattern shown here for example, and see whether there are gaseous spurs or arms which do not correspond to stellar features and whether they correspond to observed features in CO. Such features could arise from the shearing of clouds in the spiral arms (Kim & Ostriker 2002; Dobbs & Bonnell 2006) or resonances in the disc (Patsis et al. 1997; Chakrabarti et al. 2003; Martos et al. 2004).

5 ACKNOWLEDGMENTS

We thank the referee Tyler Foster for suggestions that have substantially improved the paper. We are very grateful to Nemesio Rodriguez for providing the CO velocity longitude plot from Rodriguez-Fernandez & Combes (2008), and to Tom Dame for providing the CO velocity-longitude data used for our comparison tests. We also thank Panos Patsis for valuable discussions. CLD acknowledges funding from the European Research Council for the FP7 ERC starting grant project LOCALSTAR.

REFERENCES

Baba J., Saitoh T. R., Wada K., 2010, PASJ, 62, 1413
 Benjamin R. A., 2008, in H. Beuther, H. Linz, & T. Henning ed., Massive Star Formation: Observations Confront Theory Vol. 387 of Astronomical Society of the Pacific

Conference Series, The Spiral Structure of the Galaxy: Something Old, Something New.... pp 375–+
 Binney J., Gerhard O. E., Stark A. A., Bally J., Uchida K. I., 1991, MNRAS, 252, 210
 Binney J., Tremaine S., 1987, Galactic dynamics. Princeton, NJ, Princeton University Press, 1987, 747 p.
 Chakrabarti S., Laughlin G., Shu F. H., 2003, ApJ, 596, 220
 Churchwell E., Babler B. L., Meade M. R., Whitney B. A., Benjamin R., Indebetouw R., Cyganowski C., Robitaille T. P., Povich M., Watson C., Bracker S., 2009, PASP, 121, 213
 Clemens D. P., 1985, ApJ, 295, 422
 Cohen R. S., Thaddeus P., 1977, ApJL, 217, L155
 Dame T. M., Hartmann D., Thaddeus P., 2001, ApJ, 547, 792
 Dame T. M., Thaddeus P., 2011, ApJL, 734, L24+
 Dobbs C. L., Bonnell I. A., 2006, MNRAS, 367, 873
 Dobbs C. L., Theis C., Pringle J. E., Bate M. R., 2010, MNRAS, 403, 625
 Drimmel R., 2000, A&A, 358, L13
 Englmaier P., Gerhard O., 1999, MNRAS, 304, 512
 Gittins D. M., Clarke C. J., 2004, MNRAS, 349, 909
 Kim W., Ostriker E. C., 2002, ApJ, 570, 132
 Lin L.-H., Yuan C., Buta R., 2008, ApJ, 684, 1048
 Martos M., Hernandez X., Yáñez M., Moreno E., Pichardo B., 2004, MNRAS, 350, L47
 Patsis P. A., Grosbol P., Hiotelis N., 1997, A&A, 323, 762
 Reid M. J., Menten K. M., Zheng X. W., Brunthaler A., Moscadelli L., Xu Y., Zhang B., Sato M., Honma M., Hirota T., Hachisuka K., Choi Y. K., Moellenbrock G. A., Bartkiewicz A., 2009, ApJ, 700, 137
 Rodriguez-Fernandez N. J., Combes F., 2008, A&A, 489, 115
 Roman-Duval J., Jackson J. M., Heyer M., Rathborne J., Simon R., 2010, ApJ, 723, 492
 Russeil D., 2003, A&A, 397, 133
 Stecker F. W., Solomon P. M., Scoville N. Z., Ryter C. E., 1975, ApJ, 201, 90
 Steiman-Cameron T. Y., Wolfire M., Hollenbach D., 2010, ApJ, 722, 1460
 Vallée J. P., 2005, AJ, 130, 569
 Vallée J. P., 2008, ApJ, 681, 303
 Wada K., Norman C. A., 2001, ApJ, 547, 172
 Xu Y., Reid M. J., Zheng X. W., Menten K. M., 2006, Science, 311, 54

This paper has been typeset from a \TeX / \LaTeX file prepared by the author.